



Cite this: RSC Adv., 2017, 7, 47619

Received 31st August 2017
Accepted 3rd October 2017DOI: 10.1039/c7ra09693c
rsc.li/rsc-advances

Chemical conversions using light energy have been performed in various fields since the discovery of the Honda–Fujishima effect.^{1–25} Significant efforts have recently been devoted to H₂ production by water splitting using inexhaustible light for clean energy conversion processes.^{1–4,8–29} Photoelectrode systems are widely recognised as a promising technology for H₂ production because they operate at an electrolysis voltage lower than the theoretical electrolysis voltage of water (<1.23 V).^{1,8–29} Visible light-responsive oxide photoanodes with a narrow bandgap energy, such as WO₃, BiVO₄ and Fe₂O₃, are desirable for the efficient utilisation of solar light and economical synthetic processes.^{8–29} Most importantly, numerous efforts have been focused on BiVO₄ photoanodes capable of utilising a wide range of light energy (~520 nm) and achieving efficient O₂ generation by water splitting.^{9–21,28,29,32} A WO₃/BiVO₄ photoanode that combines BiVO₄ with a WO₃ underlayer for the efficient transfer of excited electrons on BiVO₄ to the F-doped SnO₂ conductive glass (FTO) substrate shows exceptional photoelectrochemical performance for water splitting into H₂ and O₂.^{10–13,17–20,28,29,32} However, most previous investigations, containing electrochemical reactions, focused solely on the recovery of H₂ energy generated on the cathode and little attention was paid to the recovery of the oxidation products simultaneously evolved during water splitting.^{24–31}

^aResearch Center for Photovoltaics (RCPV), National Institute of Advanced Industrial Science and Technology (AIST), Central 5, 1-1-1 Higashi, Tsukuba, Ibaraki 305-8565, Japan. E-mail: k.sayama@aist.go.jp

^bDepartment of Pure and Applied Chemistry, Tokyo University of Science, 2641 Yamasaki, Noda, Chiba 278-8514, Japan

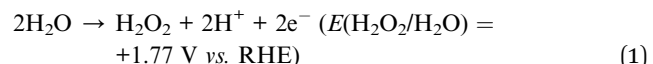
† Electronic supplementary information (ESI) available: Experimental section, SEM images, XRD spectra, LHE spectra, applied voltage properties, *I*–*V* characteristic of photoanodes, pore size distribution of the MeO_x particles, effect of Al₂O₃ amount on WO₃/BiVO₄ and dependence of applied voltage. See DOI: 10.1039/c7ra09693c

WO₃/BiVO₄ photoanode coated with mesoporous Al₂O₃ layer for oxidative production of hydrogen peroxide from water with high selectivity†

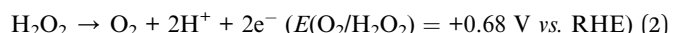
Kojiro Fuku, ^a Yuta Miyase, ^{ab} Yugo Miseki, ^a Takahiro Gunji^{ab} and Kazuhiro Sayama^{*ab}

A WO₃/BiVO₄ photoanode coated with various metal oxides demonstrated high selectivity (faradaic efficiency) for hydrogen peroxide (H₂O₂) generation from water (H₂O) under irradiation of simulated solar light in a highly concentrated hydrogen carbonate (KHCO₃) aqueous solution. A mesoporous and amorphous aluminium oxide (Al₂O₃) layer significantly facilitated inhibition of the oxidative degradation of generated H₂O₂ into oxygen (O₂) on the photoanode, resulting in unprecedented H₂O₂ selectivity (ca. 80%) and the accumulation (>2500 μM at 50C).

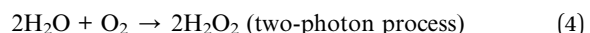
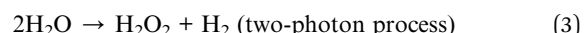
H₂O₂ is an especially versatile and clean oxidation product having the potential to generate instead of O₂ from H₂O (eqn (1)).



However, the accumulation of H₂O₂, generated oxidatively is extremely difficult because degradation of H₂O₂ into O₂ also occurs easily and oxidatively in a conventional photoelectrochemical system *i.e.* the redox potential of H₂O₂ degradation is more negative than the redox potential of H₂O₂ production from H₂O (eqn (1) and (2)), resulting in low selectivity for oxidative H₂O₂ generation.



Recently, we reported that a photoelectrochemical system combining the WO₃/BiVO₄ photoanode and aqueous electrolyte of KHCO₃ under CO₂ bubbling could achieve simultaneous generation and accumulation of H₂O₂ and H₂ from H₂O (eqn (3)).^{28,29} In this system, the aqueous electrolyte of KHCO₃ acts as an excellent oxidative catalyst for generating H₂O₂ from H₂O. Moreover, H₂O₂ could be produced at no external bias on both a WO₃/BiVO₄ photoanode (from H₂O) and an Au cathode (from O₂) *via* a two-photon process (eqn (4)).²⁹



Although the selectivity (faradaic efficiency: $\eta(\text{H}_2\text{O}_2)$) of reductive H₂O₂ production from O₂ on cathodes such as Au was very high, almost 100%, the maximum selectivity ($\eta(\text{H}_2\text{O}_2)$) for oxidative H₂O₂ production on WO₃/BiVO₄ photoanodes was still

low, only *ca.* 54%. The design of novel photoanodes capable of achieving efficient H_2O_2 generation and inhibiting oxidative degradation of generated H_2O_2 is absolutely imperative for building a clean and breakthrough technology, by accumulating H_2O_2 and H_2 with unprecedented H_2O_2 selectivity using only H_2O as the raw material.

Here, we focused on a surface modification of the metal oxide (MeO_x) layers on the $\text{WO}_3/\text{BiVO}_4$ photoanode surface to achieve excellent selectivity of generation and accumulation of H_2O_2 in the KHCO_3 aqueous solution under simulated solar light irradiation (Fig. 1). The MeO_x layers were prepared by spin-coating of metal organic solutions and calcination. Introducing a porous Al_2O_3 layer was found to specifically permit oxidative H_2O_2 generation and accumulation with exceptional selectivity in an aqueous KHCO_3 electrolyte because of the blocking effect of oxidative degradation of the generated H_2O_2 into O_2 on the photoanode.

Details regarding experimental procedures for preparation and photoelectrochemical reactions of photoanodes are provided in the ESI†.

The effects of MeO_x layers, modified on the $\text{WO}_3/\text{BiVO}_4$ photoanode, for oxidative H_2O_2 generation properties were investigated at an applied electric charge of 0.9C (900 s at steady photocurrent of 1 mA) in a 0.5 M KHCO_3 aqueous electrolyte. As shown in Fig. 2, all MeO_x -coated photoanodes, except CoO_x , enhanced the oxidative H_2O_2 generation compared to a bare $\text{WO}_3/\text{BiVO}_4$ photoanode, and the enhanced effect, ranked by the modified metal oxide, was $\text{Al}_2\text{O}_3 > \text{ZrO}_2 > \text{TiO}_2 > \text{SiO}_2 \gg \text{CoO}_x$. Little H_2O_2 was observed on the CoO_x coated photoanode, because CoO_x probably decomposed the generated H_2O_2 quickly, or O_2 may be evolved on CoO_x directly. It should be noted that the Al_2O_3 modification on the $\text{WO}_3/\text{BiVO}_4$ photoanode achieved roughly twice the oxidative H_2O_2 generation compared to the bare $\text{WO}_3/\text{BiVO}_4$ photoanode. The Al_2O_3 uniformly, smoothly and flatly covered the entire area of the $\text{WO}_3/\text{BiVO}_4$ photoanode as shown in the SEM images (Fig. 3), whereas other MeO_x were granularly and uniformly supported on that and possessed any crack holes (Fig. S1; ESI†). It was also confirmed, from XRD measurement (Fig. S2; ESI†), that no

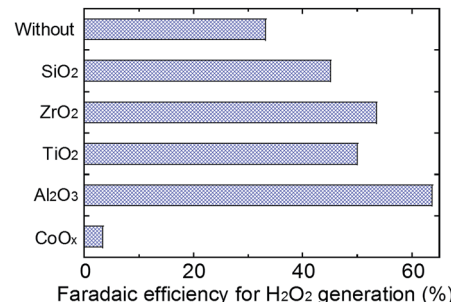


Fig. 2 Oxidative H_2O_2 generation on photoanodes ($\text{WO}_3/\text{BiVO}_4/\text{MeO}_x$) modified various metal oxides on a $\text{WO}_3/\text{BiVO}_4$ at an electric charge of 0.9C (900 s at steady photocurrent of 1 mA) in a 0.5 M KHCO_3 aqueous electrolyte (35 mL) in an ice bath (below 5 °C) under simulated solar light.

diffraction peaks derived from MeO_x were observed in all $\text{WO}_3/\text{BiVO}_4/\text{MeO}_x$ photoanodes, suggesting that all tried MeO_x modified on $\text{WO}_3/\text{BiVO}_4$ photoanode possess amorphous-like structure. As shown in Fig. S3; ESI† little change of the light harvesting efficiency (LHE) was also confirmed in tried all photoanodes, suggesting that these MeO_x introduced on the $\text{WO}_3/\text{BiVO}_4$ have little effect to light absorption efficiency on $\text{WO}_3/\text{BiVO}_4$ photoanode. The time courses of voltages applied between photoanode and a counter electrode of Pt mesh at steady photocurrent of 1 mA (Fig. 2) in oxidative H_2O_2 generation reaction were also confirmed (Fig. S4; ESI†). The voltages for applying steady photocurrent of 1 mA slightly increased by introducing MeO_x on the $\text{WO}_3/\text{BiVO}_4$ photoanode. In particular, $\text{WO}_3/\text{BiVO}_4/\text{Al}_2\text{O}_3$ photoanode, coated uniformly, smoothly and flatly at Al_2O_3 compared to other MeO_x , required highest applied voltage. In order to confirm the effect introducing the Al_2O_3 on the photoanode in more detail, the photocurrent property of the $\text{WO}_3/\text{BiVO}_4/\text{Al}_2\text{O}_3$ photoanode was investigated in a 0.5 M KHCO_3 aqueous solution (Fig. S5; ESI†). The bare $\text{WO}_3/\text{BiVO}_4$ photoanode exhibited excellent photocurrent property in all applied voltage ranges as with our past reported example,^{11,12,28,29} and the photocurrent property slightly decreased by introducing the Al_2O_3 layer. However, it should be noted that the decreasing degree of the photocurrent property was slight, only *ca.* 9% and 5% at +1.23 V and +1.77 V *vs.* RHE, respectively, although the Al_2O_3 , having an insulation property, covered the entire area of the $\text{WO}_3/\text{BiVO}_4$ photoanode. A similar

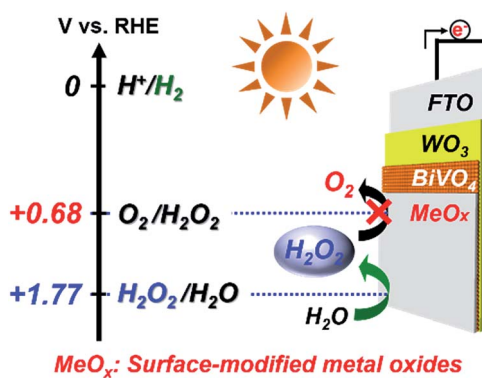


Fig. 1 Pattern and energy diagrams for photoelectrochemical H_2O_2 generation from H_2O on $\text{WO}_3/\text{BiVO}_4/\text{MeO}_x$ photoanodes under solar light irradiation.

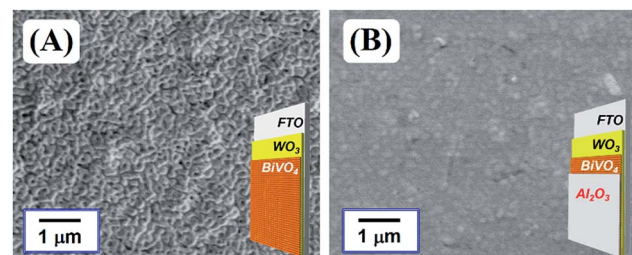


Fig. 3 SEM images of (A) $\text{WO}_3/\text{BiVO}_4$ and (B) $\text{WO}_3/\text{BiVO}_4/\text{Al}_2\text{O}_3$ photoanodes.



phenomenon has also been observed in O_2 and H_2 generation through water splitting on a photoanode coated with amorphous-like Ta_2O_5 .³² In addition, it was confirmed, from the N_2 absorption and desorption measurement of MeO_x particles (Fig. S6; ESI†), that almost all MeO_x possess mesoporous structure at a pore size of *ca.* 4–20 nm. In particular, a pore size of the Al_2O_3 was *ca.* 4.7 nm. The thicknesses of Al_2O_3 calculated from the coating amount on the $WO_3/BiVO_4$ photoanode by XRF measurement were *ca.* 100 nm (0.055 mg cm^{−2}). In order to also investigate the effects of dense Al_2O_3 on $WO_3/BiVO_4$ on the oxidative H_2O_2 generation, increasing Al_2O_3 amount on $WO_3/BiVO_4$ photoanode was performed by decreasing the spin coating number (500 rpm) of precursor solution of EMOD solved in butyl acetate containing ethylcellulose when introducing Al_2O_3 layers. The thickness of Al_2O_3 introduced at 500 rpm calculated from the XRF measurement was *ca.* 127 nm (0.070 mg cm^{−2}), suggested that the thickness increases with decreasing the spin coating number. As shown in Fig. S7; ESI† little change of the H_2O_2 generation amounts was observed on these $WO_3/BiVO_4/Al_2O_3$ photoanodes prepared at 500 and 1000 rpm, indicating that increasing Al_2O_3 on $WO_3/BiVO_4$ photoanode has little effect on the oxidative H_2O_2 generation. In subsequent experiments, $WO_3/BiVO_4/Al_2O_3$ photoanode prepared at 1000 rpm was utilized as the photoanode. These results indicate that the specific effect enhancing oxidative H_2O_2 generation property was achieved on the $WO_3/BiVO_4$ though the mesoporous and amorphous Al_2O_3 layer covered uniformly, smoothly and flatly the entire area.

To track the specific performance enhancing effect of generating H_2O_2 by introducing the Al_2O_3 layer, the concentration dependency of $KHCO_3$ aqueous electrolytes on the oxidative H_2O_2 generation property was investigated at an applied electric charge of 0.9C (Fig. 4(A)). We have already reported that the oxidative H_2O_2 generation property on the $WO_3/BiVO_4$ photoanode was improved with increasing concentration of $KHCO_3$, which acts as an effective catalyst for H_2O_2

generation *via* the two-electron oxidation of H_2O .²⁸ Even in the case of using the $WO_3/BiVO_4/Al_2O_3$ photoanode, the selectivity ($\eta(H_2O_2)$) for H_2O_2 generation was significantly enhanced with increasing concentration of $KHCO_3$, and the $\eta(H_2O_2)$ in the 2.0 M $KHCO_3$ aqueous solution reached *ca.* 80% at 0.9C, whereas that using the bare $WO_3/BiVO_4$ photoanode was *ca.* 54%. It should be noted that the selectivity ($\eta(H_2O_2) = ca. 53\%$) on the $WO_3/BiVO_4/Al_2O_3$ photoanode in lowly concentrated $KHCO_3$ (0.1 M) was comparable to that (*ca.* 54%) on the bare $WO_3/BiVO_4$ photoanode in highly concentrated $KHCO_3$ (2.0 M). This suggests that the Al_2O_3 could effectively be contributing to oxidative H_2O_2 generation from H_2O even in the lowly concentrated $KHCO_3$. Moreover, as shown in Fig. 4(B), the excellent H_2O_2 generation property on the $WO_3/BiVO_4/Al_2O_3$ photoanode compared to the $WO_3/BiVO_4$ photoanode was significantly maintained even at high electric charge up to 50C. As a result, the accumulation amount, using the $WO_3/BiVO_4/Al_2O_3$ photoanode, reached *>2500* μ M at 50C, while that using the bare $WO_3/BiVO_4$ photoanode was *>1300* μ M at 50C. The dependency of the applied voltage on the oxidative H_2O_2 generation was investigated to confirm the effect of the Al_2O_3 coating in detail (Fig. S8; ESI†). A small change in H_2O_2 generation performance was observed in all ranges of applied voltages (0.8–1.8 V), suggesting that the enhanced effect of introducing an Al_2O_3 layer is independent of the voltages applied between a photoanode as the working electrode and a Pt mesh as counter electrode using the aqueous electrolyte of the $KHCO_3$.

Although little development with regards to highly selective H_2O_2 generation *via* two-photon oxidation of H_2O and accumulation using photoanodes has been reported, our method of Al_2O_3 coating on the $WO_3/BiVO_4$ photoanode produced tremendous improvement in selective H_2O_2 generation and accumulation from H_2O in a $KHCO_3$ aqueous electrolyte. It is speculated that the specific enhancement of selectivity for H_2O_2 generation on the $WO_3/BiVO_4/Al_2O_3$ photoanode may be caused by a blocking effect, on the mesoporous Al_2O_3 layer, that inhibits oxidative H_2O_2 degradation into O_2 on the $BiVO_4$. To investigate the blocking effect on the Al_2O_3 layer, a degradation property test of H_2O_2 was performed in a 2.0 M $KHCO_3$ aqueous solution containing H_2O_2 (550 μ M) in the presence of the bare $WO_3/BiVO_4$ or $WO_3/BiVO_4/Al_2O_3$ photoanodes in presence or absence of simulated solar light irradiation in an ice bath (below 5 °C). In both cases, as shown in Fig. 5, almost all the initial amount of H_2O_2 was maintained in the dark condition, however, the H_2O_2 amount drastically decreased with irradiation by simulated solar light, suggesting that the H_2O_2 was decomposed by photocarriers (excited electrons and holes) produced on the $BiVO_4$. It should be noted that the H_2O_2 degradation in the presence of the $WO_3/BiVO_4/Al_2O_3$ photoanode was dramatically inhibited compared to the degradation in the presence of a bare $WO_3/BiVO_4$ photoanode. The oxidative H_2O_2 generation test was also confirmed in a 2.0 M $KHCO_3$ aqueous electrolyte, initially containing H_2O_2 (210 μ M) on the bare $WO_3/BiVO_4$ and $WO_3/BiVO_4/Al_2O_3$ photoanodes, to track the generated H_2O_2 degradation behaviour in more detail (Fig. 6). The generated rates of H_2O_2 were reduced by the initial addition of H_2O_2 in both cases of presence or absence of Al_2O_3 .

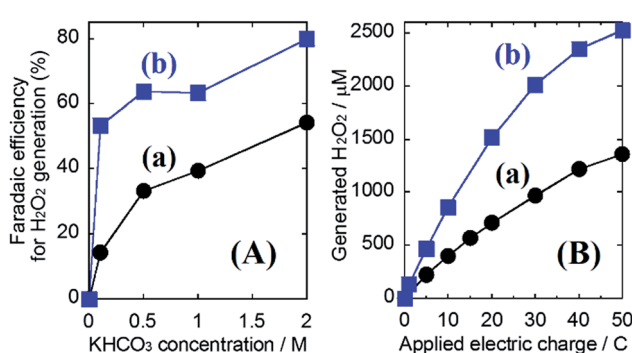


Fig. 4 (A) Oxidative H_2O_2 generation in $KHCO_3$ aqueous electrolytes (35 mL) of different concentrations at applied electric charges of 0.9C (900 s at steady photocurrent of 1 mA) under simulated solar light and (B) accumulation of oxidative H_2O_2 generation in a 2.0 M $KHCO_3$ aqueous solution (35 mL) under visible light irradiation ($\lambda > 420$ nm) using an intense Xe lamp at an applied voltage of 1.5 V in an ice bath (below 5 °C) on (a) bare $WO_3/BiVO_4$ and (b) $WO_3/BiVO_4/Al_2O_3$ photoanodes.



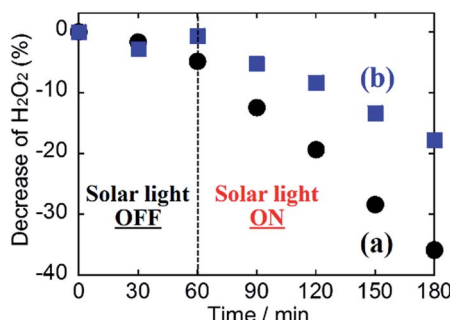


Fig. 5 Degradation properties of H_2O_2 (550 μM) initially added in a 2.0 M KHCO_3 aqueous solution in an ice bath (below 5 $^{\circ}\text{C}$) under CO_2 bubbling and simulated solar light irradiation in the presence of (a) $\text{WO}_3/\text{BiVO}_4$ and (b) $\text{WO}_3/\text{BiVO}_4/\text{Al}_2\text{O}_3$ photoanodes at no applied voltage.

However, the decreasing rate of H_2O_2 generation was significantly inhibited, from *ca.* 61% to *ca.* 39%, by introducing the Al_2O_3 layer on the $\text{WO}_3/\text{BiVO}_4$ photoanode. These results suggest that introducing the Al_2O_3 layer significantly contributed to the highly selective H_2O_2 generation and accumulation from H_2O , with a high photocurrent property, by a blocking effect that inhibited the oxidative degradation of generated H_2O_2 . The mechanism of blocking effect is proposed that the H_2O_2 generated on the BiVO_4 in the $\text{WO}_3/\text{BiVO}_4/\text{Al}_2\text{O}_3$ photoanode diffuses in electrolyte of KHCO_3 aqueous solution through mesoporous of the Al_2O_3 , and contact of the H_2O_2 diffused in electrolyte with the BiVO_4 covered uniformly and smoothly Al_2O_3 may be significantly inhibited compared with that with bare BiVO_4 , resulting in the formation of effective inhibition of oxidative H_2O_2 degradation. Furthermore, there may be other possible mechanisms such as a blocking effect of a direct O_2 evolution site *via* a 4-photon process covering by Al_2O_3 , or an enrichment effect resulting from the increasing KHCO_3 concentration around the photoanode based on the acid-base adsorption between HCO_3^- (a weak base) and the weakly acidic sites on the Al_2O_3 surface, related to the good

$\eta(\text{H}_2\text{O}_2)$ in lower KHCO_3 concentration, as shown in Fig. 4(A). The tracking and contribution of these other mechanisms, on the Al_2O_3 layer, is currently under investigation.

Conclusions

In summary, various metal oxides were coated onto a $\text{WO}_3/\text{BiVO}_4$ photoanode to enhance the selectivity (faradaic efficiency) of oxidative H_2O_2 generation, in an aqueous electrolyte of KHCO_3 , from water under solar light irradiation. Among the various metal oxides, the Al_2O_3 coating, which produced a mesoporous and amorphous structure on the $\text{WO}_3/\text{BiVO}_4$ photoanode, achieved excellent oxidative H_2O_2 generation at a selectivity of *ca.* 80% and an accumulation of $>2500 \mu\text{M}$ (50C). Interestingly, the Al_2O_3 -coated $\text{WO}_3/\text{BiVO}_4$ photoanode dramatically inhibited oxidative degradation of H_2O_2 generated on the $\text{WO}_3/\text{BiVO}_4$ photoanode after introducing the Al_2O_3 layer. This study contributes to developing a promising design for a clean H_2O_2 production system that uses only water as the raw material under solar light irradiation. More effective dreamy H_2O_2 generation, at an excellent selectivity close to 100%, can be expected by modifying the surface-treatment technology, and it is currently under investigation.

Conflicts of interest

There are no conflicts to declare.

Acknowledgements

The present work was partially supported by JSPS KAKENHI Grant Number 26810105 and the International Joint Research Program for Innovative Energy Technology. We thank Dr Etsuko Fujita (Brookhaven National Laboratory) for helpful discussions.

Notes and references

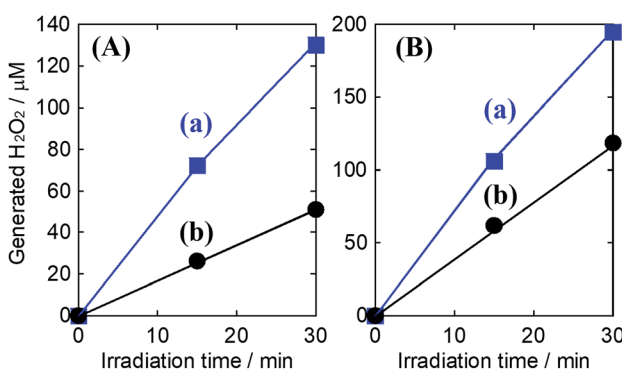


Fig. 6 Comparison of oxidative H_2O_2 generation in a 2.0 M KHCO_3 aqueous electrolyte (a) in the absence of or (b) containing initially-added H_2O_2 (210 μM) in an ice bath (below 5 $^{\circ}\text{C}$) on a (A) $\text{WO}_3/\text{BiVO}_4$ and (B) $\text{WO}_3/\text{BiVO}_4/\text{Al}_2\text{O}_3$ photoanodes under simulated solar light irradiation at steady photocurrent of 1 mA.

- 1 A. Fujishima and K. Honda, *Nature*, 1972, **238**, 37.
- 2 Z. G. Zou, J. H. Ye, K. Sayama and H. Arakawa, *Nature*, 2001, **414**, 625.
- 3 A. Kudo and Y. Miseki, *Chem. Soc. Rev.*, 2009, **38**, 253.
- 4 K. Maeda, K. Teramura, D. Lu, T. Takata, N. Saito, Y. Inoue and K. Domen, *Nature*, 2006, **440**, 295.
- 5 K. Fuku, K. Hashimoto and H. Kominami, *Chem. Commun.*, 2010, **46**, 5118.
- 6 K. Fuku, T. Kamegawa, K. Mori and H. Yamashita, *Chem.-Asian J.*, 2012, **7**, 1366.
- 7 K. Fuku, R. Hayashi, S. Takakura, T. Kamegawa, K. Mori and H. Yamashita, *Angew. Chem., Int. Ed.*, 2013, **52**, 7446.
- 8 B. D. Alexander, P. J. Kulesza, I. Rutkowska, R. Solarska and J. Augustynski, *J. Mater. Chem.*, 2008, **18**, 2298.
- 9 K. Sayama, A. Nomura, Z. Zou, R. Abe, Y. Abe and H. Arakawa, *Chem. Commun.*, 2003, 2908.
- 10 P. Chatchai, Y. Murakami, S. Kishioka, A. Y. Nosaka and Y. Nosaka, *Electrochim. Acta*, 2009, **54**, 1147.



11 R. Saito, Y. Miseki and K. Sayama, *Chem. Commun.*, 2012, **48**, 3833.

12 I. Fujimoto, N. Wang, R. Saito, Y. Miseki, T. Gunji and K. Sayama, *Int. J. Hydrogen Energy*, 2014, **39**, 2454.

13 X. Shi, I. Y. Choi, K. Zhang, J. Kwon, D. Y. Kim, J. K. Lee, S. H. Oh, J. K. Kim and J. H. Park, *Nat. Commun.*, 2014, **5**, 4775.

14 T. W. Kim and K. S. Choi, *Science*, 2014, **343**, 990.

15 Y. Liu, Y. Guo, L. T. Schelhas, M. Li and J. W. Ager III, *J. Phys. Chem. C*, 2016, **120**, 23449.

16 L. H. Hess, J. K. Cooper, A. Loiudice, C. M. Jiang, R. Buonsanti and I. D. Sharp, *Nano Energy*, 2017, **34**, 375.

17 J. Su, L. Guo, N. Bao and C. A. Grimes, *Nano Lett.*, 2011, **11**, 1928.

18 P. M. Rao, L. Cai, C. Liu, I. S. Cho, C. H. Lee, J. M. Weisse, P. Yang and X. Zheng, *Nano Lett.*, 2014, **14**, 1099.

19 I. Grigioni, K. G. Stamplecoskie, D. H. Jara, M. V. Dozzi, A. Oriana, G. Cerullo, P. V. Kamat and E. Selli, *ACS Energy Lett.*, 2017, **2**, 1362.

20 K. Mase, M. Yoneda, Y. Yamada and S. Fukuzumi, *ACS Energy Lett.*, 2016, **1**, 913.

21 F. M. Toma, J. K. Cooper, V. Kunzelmann, M. T. McDowell, J. Yu, D. M. Larson, N. J. Borys, C. Abelyan, J. W. Beeman, K. M. Yu, J. Yang, L. Chen, M. R. Shaner, J. Spurgeon, F. A. Houle, K. A. Persson and I. D. Sharp, *Nat. Commun.*, 2016, **7**, 12012.

22 J. Y. Kim, G. Magesh, D. H. Youn, J. W. Jang, J. Kubota, K. Domen and J. S. Lee, *Sci. Rep.*, 2013, **3**, 2681.

23 Q. Mi, A. Zhanaidarova, B. S. Brunschwig, H. B. Gray and N. S. Lewis, *Energy Environ. Sci.*, 2012, **5**, 5694.

24 J. C. Hill and K. S. Choi, *J. Phys. Chem. C*, 2012, **116**, 7612.

25 K. Ueno and H. Misawa, *NPG Asia Mater.*, 2013, **5**, e61.

26 K. Fuku, N. Wang, Y. Miseki, T. Funaki and K. Sayama, *ChemSusChem*, 2015, **8**, 1593.

27 H. G. Cha and K. S. Choi, *Nat. Chem.*, 2015, **7**, 328.

28 K. Fuku and K. Sayama, *Chem. Commun.*, 2016, **52**, 5406.

29 K. Fuku, Y. Miyase, Y. Miseki, T. Funaki, T. Gunji and K. Sayama, *Chem.-Asian J.*, 2017, **12**, 1111.

30 K. Fuku, Y. Miyase, Y. Miseki, T. Gunji and K. Sayama, *ChemistrySelect*, 2016, **1**, 5721.

31 T. Shiragami, H. Nakamura, J. Matsumoto, M. Yasuda, Y. Suzuri, H. Tachibana and H. Inoue, *J. Photochem. Photobiol. A*, 2015, **313**, 131.

32 R. Saito, Y. Miseki, W. Nini and K. Sayama, *ACS Comb. Sci.*, 2015, **17**, 592.

